Mode structure of a Transparent Cathode Discharge

T. Hardiment, M. D. Bowden

Abstract— **In this study we characterize a Transparent Cathode Discharge, a type of Inertial Electrostatic Confinement plasma, operated in helium and argon in the pressure range of 1~100 Pa. The discharge was investigated using a combination of electrical and optical diagnostic techniques. Imaging of the discharge indicated distinct operating regimes related to the background gas pressure, with each mode being characterized by different patterns of optical emission. Spectroscopic analysis of the optical emission showed that this mode structure represented an electron-driven discharge at higher pressures, and a discharge sustained by the activity of energetic heavy particles at lower pressures. The higher-pressure discharge is shown to be assisted by the hollow cathode effect towards its low-pressure limit, and the visible color of emission from the discharge in helium is found to provide a convenient diagnosis of active species. The identification of a stable discharge mode in which energetic heavy particles are responsible for collisional processes has the potential to lead to new industrial applications based on this novel heavy particle-driven reactive plasma source.**

Index Terms— **glow discharge, hollow-cathode effect, ion-impact collision, Inertial Electrostatic Confinement, plasma**

I. Introduction

MOST laboratory and industrial plasmas are sustained by the activity of energetic electrons, whose properties determine the chemistry, temperature and general reactive profile of the plasma. The distribution of energetic electrons varies between different types of discharge, and the wide range of temperature, species composition and densities that characterize different discharges enables a wide range of applications. Discharge plasmas that contain significant populations of energetic ionic and neutral species, however, are rare. The presence of such energetic heavy particle species may affect characteristics such as gas heating and molecular fragmentation, and so the mix of reactive species in such a plasma could be quite distinct from those of conventional sources. This has the potential to either generate novel applications, or to constitute an improvement over current means of obtaining a given reactive plasma profile.

This paper was submitted for review on January 31, 2019. The work was supported in part by the Engineering and Physical Sciences Research Council.

T. Hardiment is with the Department of Electrical Engineering and Electronics, University of Liverpool, UK (e-mail: t.hardiment@liverpool.ac.uk).

M. D. Bowden is with the Department of Electrical Engineering and Electronics, University of Liverpool, UK (e-mail: mark.bowden@liverpool.ac.uk).

This paper describes an investigation of a discharge previously studied within the field of Inertial Electrostatic Confinement (IEC), and which has been referred to as a Transparent Cathode Discharge (TCD) [1]. We use the term TCD because it describes a principal aspect of the electrode configuration and because our study is carried out in the self-sustained discharge regime, unlike some other IEC work. Previous research in TCD/IEC devices has shown that these discharges contain energetic ion species. The aim of our research is to identify the major discharge regimes, understand the physical mechanisms that underlie each regime and, in particular, to determine the role of energetic ionic and neutral species.

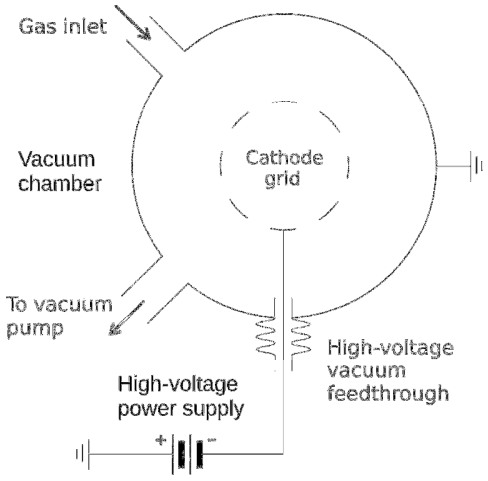

Fig. 1. Simplified schematic of TCD apparatus

The IEC concept originated in the 1950s and '60s as an approach to creating fusion plasmas by the electrostatic confinement and acceleration of ions within a negative space charge of electrons [2]-[6]. In the 1990s, the readily-achievable fusion reactivity offered by simple devices operating in the glow discharge regime led to consideration for non-power fusion applications that utilise the MeV products of fusion reactions such as neutron and protons. An industry neutron source based on a simple IEC device was considered to be the first commercial application of a fusing plasma [7], and proof-of-principle has been demonstrated as a proton source, for application in medical isotope production [8]. Interest has also been shown for spacecraft thruster applications, variously using the products of fusion [9] and

charge-exchange [10] reactions.

IEC devices have been operated in both spherical and cylindrical configurations, with electrode arrangements used in early IEC work having a central mesh grid variously as cathode or anode. The majority of more recent discharge work has been conducted using spherical grid electrodes of relatively open construction, most simply with a central cathode grid surrounded by the grounded chamber wall, as shown in Fig. 1. Discharges obtained in this configuration are generally operated at sufficiently-low pressures for path lengths to be significant fractions of the device dimension, with a cathode bias typically units to tens of kilovolts.

Charged particles created by ionisation within the inter-electrode region are accelerated by the electric field, causing electrons to flow outwards to the walls, and positive ions to be accelerated inwards. Those ions that pass through the cathode apertures are injected into the central region within the cathode. The importance of charge-exchange reactions has been noted as causing the transfer of much ion energy to neutrals, creating an outwardly-directed energetic neutral flux [11]-[13].

This paper describes the principal characteristics of a TCD operated in a cylindrical geometry, in simple atomic gases across a relatively wide range of conditions of pressure and voltage. The objective of the study is the understanding of physical processes at work within the discharge, and how these depend upon operating conditions. The experimental apparatus is described in Section 2. In Section 3, experimental observations are used to characterise the discharge in terms of its apparent mode structure, based on the results of measurements of optical emission, current-voltage relations and spectroscopically-resolved emission structure. Section 4 contains analysis directed towards the identification of species responsible for causing energetic collisions within the plasma, while Section 5 is a brief comparison of this study with those reported for similar discharges.

II. Experimental Arrangement

A. Vacuum system

The experiment is contained within a cube-shaped vacuum chamber, with 30 cm sides. The floor and walls are made from 10 mm stainless steel, and the top from acrylic. Centrally-located circular ports of similar diameter are located on opposing sides of the chamber, one pair measure 10 cm, and the other are 4 cm. A further pair of 4-cm ports are located off-centre, and one additional port is located in the centre of the chamber floor. These are used for connection of vacuum pumps, gas and electrical feed-through components and vacuum gauges, and a viewing window is fitted to one of the two larger ports. Sputtered electrode material can accumulate relatively quickly during operation at some conditions, and so glass shields are installed over port glasses to assist in maintaining optical transmission. X-rays generated by high-velocity particles impacting chamber surfaces are shielded at the window and chamber lid, using high lead-content glass.

The chamber is evacuated with a Leybold Turbovac50 turbo-molecular pump, backed by an Edwards RV3 rotary vane pump. This system provides a base pressure of around 10^{-6} Pa in the chamber. Small quantities of gas may be admitted via two MKS GE50A series mass flow controllers, with flow rates of 20 and 100 sccm and operated by means of an MKS 647C control unit. Pressures smaller than around 12 Pa are monitored by a Pfeiffer CMR375 capacitance manometer, and a Pfeiffer PCR260 dual pirani gauge is used for higher pressures, both connected to a Pfeiffer TPG control unit.

B. Electrodes

The chamber contains two cylindrical grid electrodes, arranged coaxially, with the cathode positioned inside the anode. Both electrodes have fourteen apertures around the circumference, and are made from 1.6 mm-diameter stainless steel. The cathode radius is a little less than 3 cm, half that of the anode. The cathode is 10 cm in length, and the anode is made somewhat longer by an additional row of apertures at each end, terminating at a ring of some 80 % of the main radius. These give it a barrel-shaped form, as shown in Fig. 2. The high-voltage feed-through serves as cathode support, and the anode grid is supported by a simple stainless steel stand, electrically isolated from the chamber. The cathode has a radial geometric transparency of ~0.79, and the anode ~0.86, as calculated for the portion of the electrodes corresponding to the central four rows of apertures. The anode is connected to ground via a small resistance, sufficient for a few volts to be developed across it. This enables anode current to be

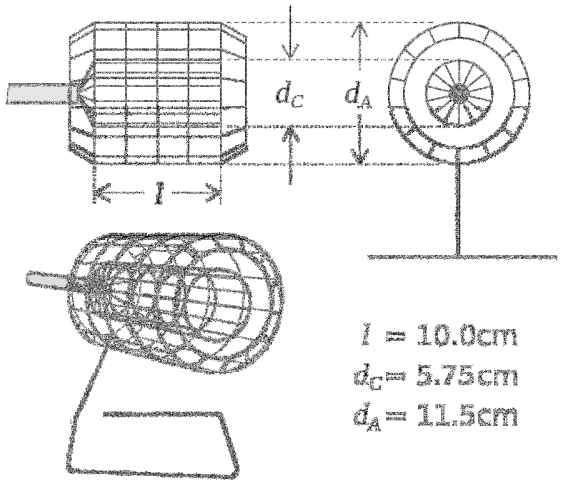

Fig. 2. The form and dimensions of the electrodes and their means of support

monitored, whilst effectively maintaining the electrode at ground potential.

C. Power supplies

The cathode is driven via a 3.9 kΩ series resistance, by one of two available Glassman WX series power supplies. These are capable of sinking 100 mA at voltages up to 10 kV, and 35 mA at 30 kV, although in practice, voltage is limited by the

feed-through arrangement to around 20 kV. These power supplies operate in either a constant-current or a constant-voltage mode, with limiting values for levels of voltage and current set manually, and the operating mode automatically selected by whichever parameter limits the output.

D. Diagnostics

For electrical measurements, a system based around the ADC function on an Arduino microcontroller was used to record the analogue monitoring signals for cathode voltage and current generated by the power supply, and also an analogue signal generated by the pressure gauge controller. The ADC is 10-bit, and so the resolution of measurements made using this system is around 0.1 % of full scale. In order to account for non-linearities in the signal paths, transfer functions were measured on the bench, and an appropriate correction applied to the recorded values.

The spectrometer used for monitoring light emitted from the plasma was a Horiba FHR1000 spectrometer, sensitive to the range of wavelengths between 250 nm and 750 nm. This was controlled so as to cause a progressive range of wavelengths to be incident upon a photo-multiplier tube, and the intensity recorded. For the measurements recorded in this study, the lead glass was not fitted to the viewport, and the sampled light was transmitted to the spectrometer via an Ocean Optics UV-Vis fibre. This system enables good transmission of most visible wavelengths, with some attenuation occurring below around 400 nm.

III. EXPERIMENTAL OBSERVATIONS

A. Overview of mode structure and distributions of emission

The spatial distribution of optical emission was observed through a series of camera images of the discharge, obtained for different values of the background gas pressure. Rather than showing a gradual evolution, the discharge emission showed a characteristic pressure-dependent mode structure. This mode structure was observed to be broadly similar in helium, neon, argon and nitrogen, and provides a convenient framework for description of discharge characteristics. The following refers to the discharge in helium.

Across the range of pressures from units to hundreds Pa, the appearance of the discharge evolves through three distinct regimes. At relatively high pressures, of a few hundred pascals, emission is generally localised within the region between the electrodes, with cathode voltages typically a few hundreds of volts. These properties resemble those of conventional glow discharges with solid electrodes, and

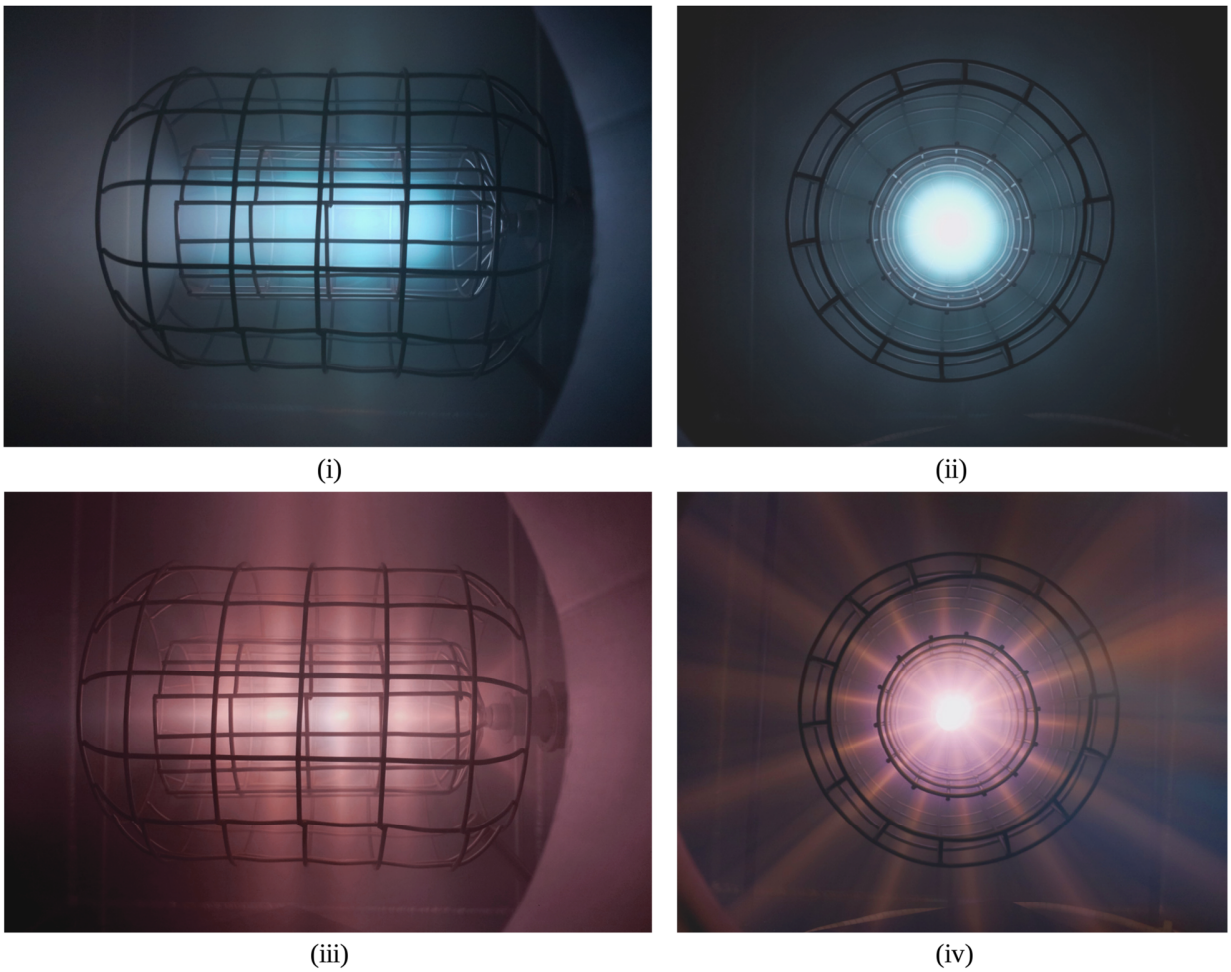

Fig. 3. Photographs of the helium discharge at i) and ii) 40 Pa; iii) and iv) 4 Pa (in colour online)

considering this state to be broadly similar, we did not investigate it further.

At pressures smaller than 100 Pa, the region of bright emission becomes principally localised to within the interior of the cathode, as shown in Fig. 3 i) and ii). This characteristic appearance is consistently evident across a range of pressures extending down to around 13 Pa, with voltages remaining smaller than 1 kV. If pressure is further reduced to units Pa, the appearance of the discharge changes again, to become a series of radial beams which pass through the apertures of both grids, converging at the central axis and extending to the walls [Fig. 3 iii) and iv)]. A glow extends from the open end of the cathode at transitional pressures (Fig. 4), and this becomes a narrow beam at lower pressures. In this regime, cathode voltage rises quickly with decreasing pressure, from around a kilovolt to tens of kilovolts, and the low-pressure limit for operation in this apparatus is determined by the available voltage.

The two lower-pressure modes occurring below 100 Pa are the main subject of this study. Of these, the mode occurring at higher pressures, in which the glow is largely confined to within the cathode, shall be referred to as the 'cathode-confined' (CC) mode [Fig. 3 i) and ii)]. That occurring at lower pressures, in which emission is localised so as to resemble radial beams, shall be referred to as the 'beam' mode [Fig. 3 iii) and iv)].

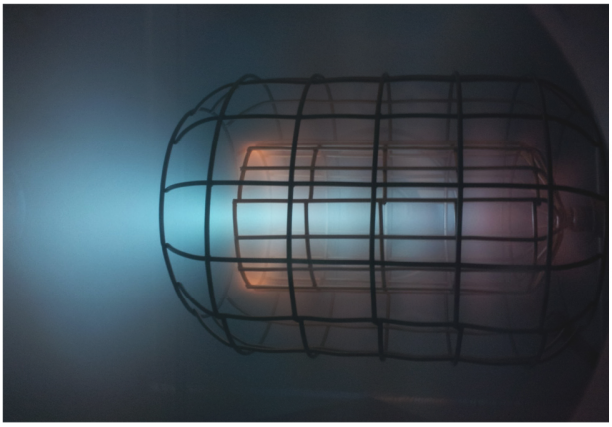

(i)

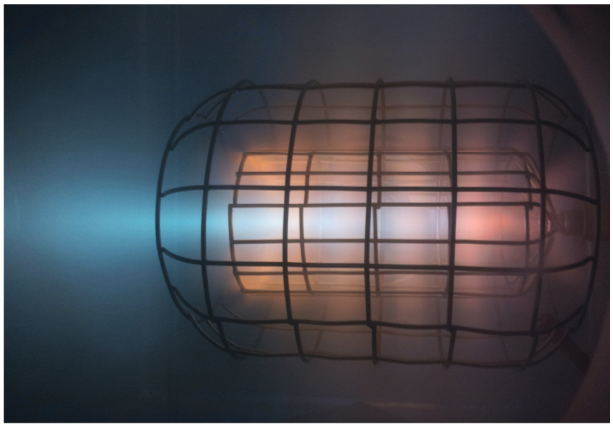

(ii)

Fig. 4. Photographs of the helium discharge at i) 15 Pa and ii) 12 Pa (in colour online)

In helium, the visible glow emitted from these two discharge modes is notably different in colour to the eye. Emission from the higher-pressure mode is blue-green in appearance, and the low-pressure beams are orange. At pressures corresponding to the mode transition, both of these colours are evident in the beam mode discharge, in the axial and radial locations chiefly occupied by the two modes. This is illustrated with photographs of emission distributions at two such pressures in Fig. 4. The emission structure is therefore observed to show an association with spatial location within the chamber.

In different gases, the evolution from cathode-confined glow to radial beams is generally similar, with the progression occurring in the helium discharge at around four times the pressure of that in argon. This broad mode structure is made additionally complex, at certain conditions, by the appearance of various additional discharge features within the cathode that might be described as 'space charge objects'. These may affect the discharge properties to varying extents, and occur over a comparatively narrow range of conditions. They are not discussed further in this paper, but will be treated in detail in future publications.

B. Current-voltage relations

Current-voltage relations were measured at conditions in which the discharge operates in both the CC and beam modes, in helium and argon. With the current limit set fully open on the power supply, the voltage was ramped up and down quite quickly, over a period of a few seconds, and values of voltage from the monitoring outputs of the power supply were sampled at a rate of around 20 Hz using the ADC system. This was found to be the best way to minimise the effects of voltage drift. The cathode voltage is obtained from the supply voltage by subtracting the voltage dropped across the ballast resistor. Levels of current were recorded similarly, in some cases using an active sensor.

The curves obtained in helium are plotted in Fig. 5, and those for argon in Fig. 7. These are colour-coded, with blue used for pressures at which the discharge remained in the beam mode. A variety of colours are used to help distinguish the CC mode curves. Occasional instabilities in the discharge cause distortion of the curves, as is visible on the argon curve recorded at 1.1 Pa, and to a lesser extent the helium curve for 11.7 Pa. Outlying values corresponding to power supply regulation have been removed for clarity.

For the helium curves (Fig. 5), the mode structure is most apparent towards the low-pressure limit of the CC mode, where the onset of the mode is indicated by significant discontinuities in current and voltage. These correspond to sudden increases in current, and are indicated by arrows for the data obtained at pressures between around 13 Pa and 32 Pa. Across this range of pressures, voltage levels also start to show a pressure-dependence that is not evident for the curves obtained at 32 Pa and 85 Pa. The threshold current for the mode is observed to become smaller with increasing pressure,

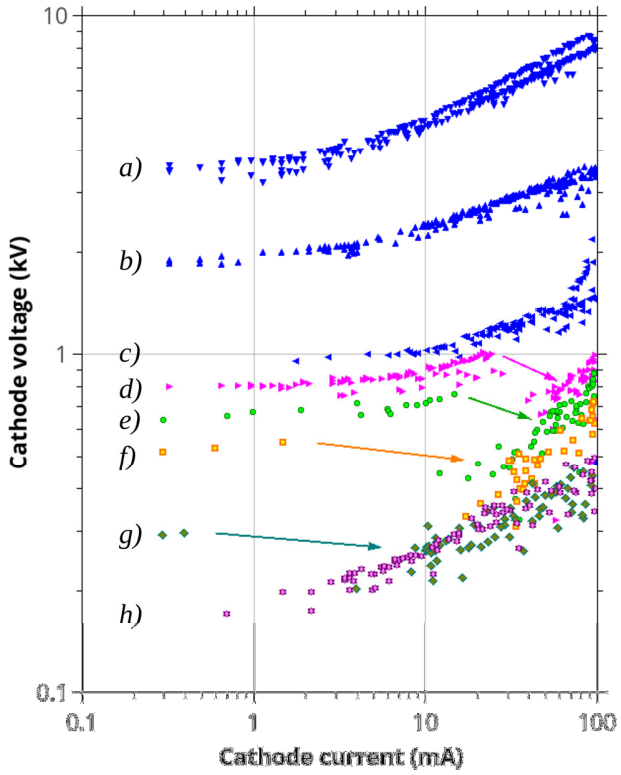

Fig. 5. I-V curves for helium discharges at pressures: a) 3.9 Pa; b) 6.1 Pa; c) 11.7 Pa; d) 12.8 Pa; e) 14.8 Pa; f) 18.7 Pa; g) 32 Pa; h) 85 Pa. Arrows indicate jumps in current and voltage on instigation of the CC mode (in colour online).

and at pressures greater than 32 Pa the CC mode appears instantaneously upon breakdown.

The curve obtained in helium at 12.8 Pa is shown in isolation in Fig. 6, to illustrate this behaviour in more detail. As voltage is increased to around 1 kV, the discharge transitions to the CC mode, at which point the current jumps from below 30 mA to above 70 mA, and voltage falls by around 20 %. As voltage is subsequently reduced, the mode

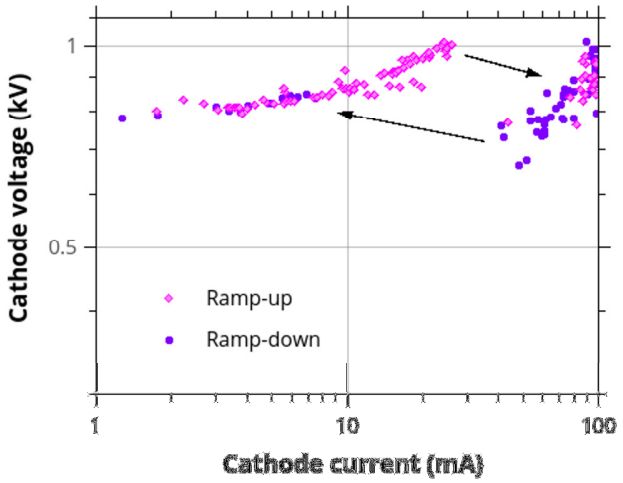

Fig. 6. I-V curve in helium for a pressure of 12.8 Pa, showing hysteresis associated with CC mode formation and extinction (in colour online)

persists to around 40 mA before it extinguishes, indicating a hysteresis to be associated with the mode.

Current-voltage curves for argon are shown in Fig. 7, with blue again used to indicate beam mode curves. Curves for the CC mode correspond to pressures greater than around 17 Pa, with similar discontinuities occurring in levels of cathode current when the mode appears at lower pressures. This may be seen most clearly in the curve for 2.9 Pa [marked iv)]. In argon, the jumps in current are accompanied by a relatively smaller change in the current-voltage trend, making the mode transition region less obvious in Fig. 7 than for the helium curves in Fig. 5. Curves for the CC mode in argon are

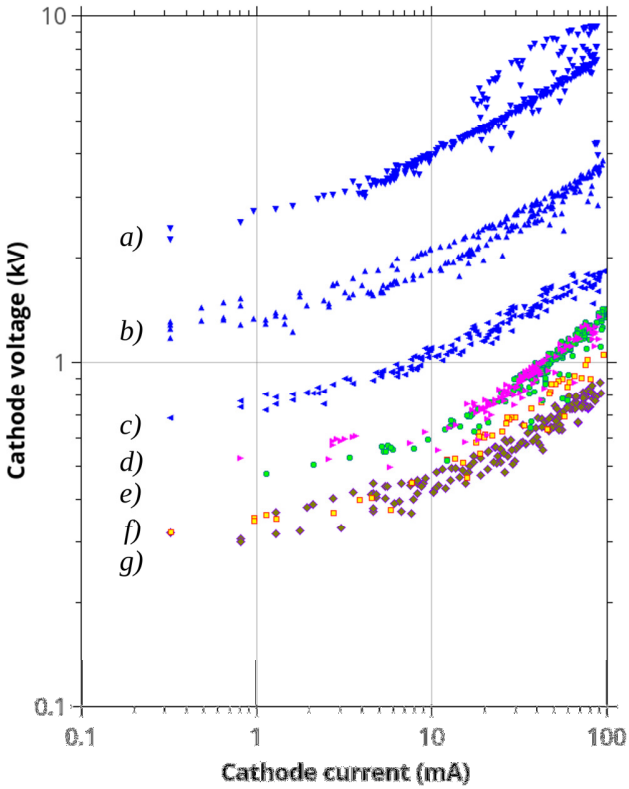

Fig. 7. I-V curves for argon discharges at pressures: a) 1.1 Pa; b) 1.7 Pa; c) 2.4 Pa; d) 2.9 Pa; e) 3.9 Pa; f) 5.7 Pa; g) 9.3 Pa (in colour online).

observed to correspond to generally higher voltages than those for helium.

C. *Optical emission spectroscopy*

Optical emission from helium discharges was spectrally resolved for the range of wavelengths between 250 nm and 750 nm. An optical fibre was aimed through a glass viewport towards the axis of the discharge, aligned with the centre of the electrode apertures, and light was sampled according to the fibre's angle of acceptance at a range of pressures between 2.5-50 Pa, across which the discharge operates in both the CC and beam modes. Prior to the making of each measurement, the discharge was allowed to reach a stable equilibrium, and voltage and pressure noted.

Characteristic spectra from i) CC and ii) beam mode discharges are shown in Fig. 8. All of the significant lines appearing in these spectra are helium lines, with the line at

501.6 nm strongest for the CC mode, and the line at 587.6 nm brightest for the beam mode. These spectral lines were found to dominate the modes' emission structure throughout their respective pressure ranges, and as light at these respective wavelengths is green and yellow-orange, they clearly

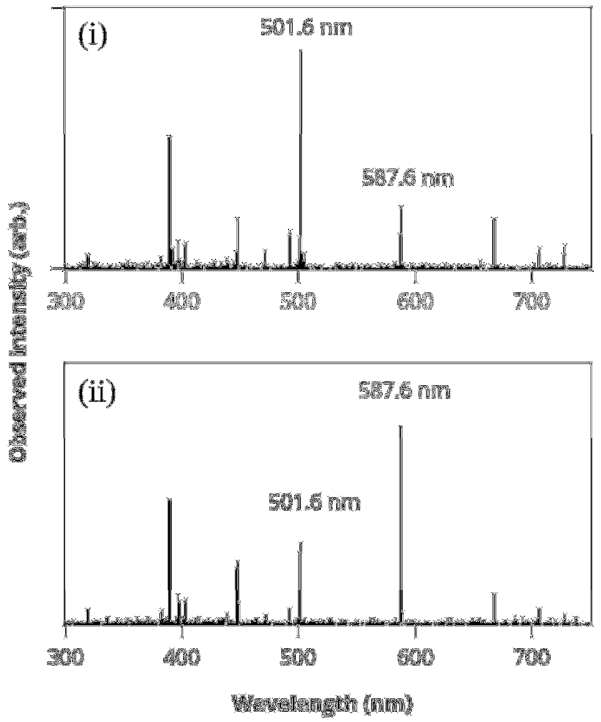

Fig. 8. Optical emission spectra from helium discharges at i) 50 Pa, 200 V (CC mode); ii) 4.3 Pa, 9 kV (beam mode).

contribute much to the visible colour of emission. The line at 388.9 nm is consistently strong in either mode.

Overall levels of emission vary considerably across the pressure range, and so in order to compare profiles recorded across a wide range of conditions, the spectra were normalised to within a set of 15 lines that consistently appear brightest

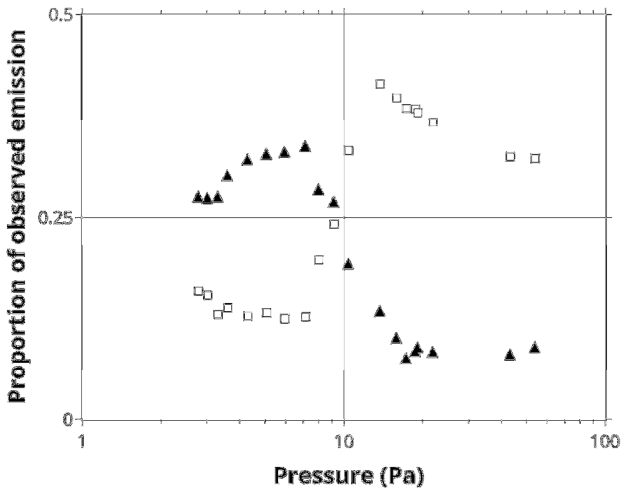

Fig. 9. Variation in relative intensities of 501.6 nm (open squares) and 587.6 nm (closed triangles) spectral lines in optical emission from the helium discharge across a range of pressures.

within the spectrum. These make up the vast majority of recorded signal, as is evident from the examples in Fig. 8.

Relative intensities of the 501.6 nm and 587.6 nm lines within this set of lines are shown against pressure in Fig. 9. The significant change associated with the mode structure is clearly apparent, at pressures between 8-15 Pa.

IV. ANALYSIS

A. *Emission structure*

Our motivation being the development of a plasma source in which processes are caused by energetic heavy particles, the identification of relevant operating regimes is of primary interest. In the following, we initially consider the emission structure in helium, since this shows such a clear association with the two discharge modes. The relation of a different, principal spectral line with each mode was noted to extend to the regions of the chamber in which these occur, and we observe these regions to also correspond to different relative strengths of electric field. This suggests a dependence upon conditions of *E/n*, for both the emission structure and the mode structure more generally.

Phelps and Jelenkovic [14] have reported that the relative intensities of the 501.6 nm and 587.6 nm helium lines may be, under some conditions, associated with a change in the collision process causing the excitation. In their experiment, they observed that, for *E/n* below 1 kTd, emission intensity towards the anode of a planar discharge increased exponentially for both wavelengths, consistent with increasing levels of excitation accompanying electron multiplication in the gap. In the cathode region, however, additional structure was observed at *E/n* between 1 kTd and 10 kTd, principally at 587.6 nm, and increasing exponentially towards the cathode. After modelling excitation processes caused by electrons, ions and fast atoms, Phelps and Jelenkovic concluded that the additional structure in the observed emission was the result of ion- and neutral- induced excitation. The contribution to 587.6 nm emission of excitation by fast atoms was found to be comparable to that from electrons at *E/n* of around 4 kTd, while the 501.6 nm emission was dominated by electron-impact processes throughout the *E/n* range to 7 kTd. The conditions of *E/n* at which the emission profile changed also agrees with analysis in [15], in which inelastic processes caused by heavy particle-impact are found to become significant at *E/n* greater than a few kTd in helium.

We do not have detailed information regarding the potential distribution within our own discharge, but values of *E/n* can be estimated that are likely to encompass real conditions. The electric field along the radial lines connecting i) cathode and anode grids, and ii) the cathode grid and chamber wall, can be approximated as full cathode potential distributed over the relevant dimensions. At the mode transition in helium, cathode voltages rise from 100s V to units kV, at pressures between 12 – 15 Pa. Ranges of *E/n* calculated for these pressures, and for voltages of 500 V and 1000 V, distributed across distances of 12 cm and 3 cm, are shown in Table 1.

The larger values are noted to correspond to conditions found in the radial region surrounding the cathode, occupied

by the beam mode discharge, but in which little emission is evident during the CC mode discharge. These agree very well with the range of conditions at which excitation by massive particles may be expected to become important, from [14] and [15]. Light is emitted at 501.6 nm and 587.6 nm in electronic transitions originating from the 3^1P and 3^3D levels of helium, and cross sections for direct excitation to these levels by ions and electrons have very different magnitudes (Fig. 10). These indeed suggest the emission structure to represent a change from electron- to ion-impact processes, but we note observed emission profiles may be significantly affected by pressure also. The experiments in [14] are made at a pressure of 1 Torr (133 Pa), constituting optically-thick conditions, and the authors observe that radiation imprisonment and excitation transfer will result in substantial increases in observed emission, relative to that caused by direct excitation, disproportionately affecting light at 587.6 nm by a factor of around 3 relative to 501.6 nm. Although made at lower pressures, our measurements are expected to be subject to a varying degree of these effects. This cannot explain our results however, since we find increased emission at 587.6 nm in the lower-pressure mode, contrary to the expected trend, and our results show a clear association with mode rather than a progressive pressure-dependence. We conclude, therefore, that the observed emission profile is representative of the underlying cross section structure at these conditions.

TABLE I
RANGES OF *E/N* CALCULATED FOR CONDITIONS TO EITHER SIDE OF MODE TRANSITION

Mode	Pressure (Pa)	Voltage (V)	Length voltage is dropped across (cm)	E/n (kTd)
CC	15	500	12 [a]	1.2
			3 [b]	4.6
Beam	12	1000	12	2.9
			3	11.5

[a]Distance between cathode and chamber wall.
[b]Distance between cathode and anode.

Ref. [15] indicates processes of ionisation caused by heavy particles to also become significant at *E/n* conditions of between 5 – 10 kTd. The mechanism behind this dependence for different species may be understood by considering cross sections for ionisation of helium by electrons and heavy particles (Fig. 11). These show quite different energy-dependences; although the threshold energies for ions and electrons are of similar order, the electron-impact cross section is peaked at ~100 eV (similar in this respect to that for excitation to 3^1P shown in Fig. 10 i), whilst the ion-impact cross section remains large at energies in the 10s keV. The cross section for neutrals does not become large until this range, but then also remains high. In a regime in which particles have relatively high energies, it is therefore the heavy species that will contribute most to ionisation. Additionally, the large difference in mass between electrons and heavy particles means these become energetic at distinct ranges of *E/n*, and so there will be a finite range of *E/n* at which

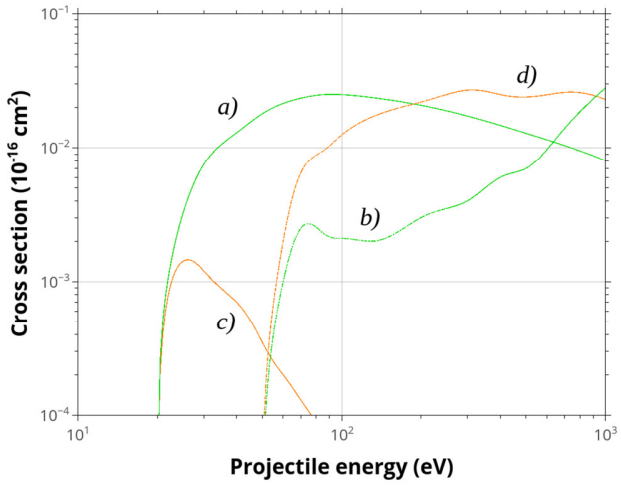

Fig. 10. Cross sections for excitation to the 3^1P level (501.6 nm) by a) electrons and b) ions, and to the 3^3D level (587.6 nm) by c) electrons and d) ions. Electron data is taken from [16]; ion data from [17].

electrons have suitable energies to cause ionisation, above which it will be principally caused by ions and neutrals.

Following our assessment of *E/n*, we may gain some idea of how this transition between active species relates to our discharge by comparing mean free paths for electron-impact ionisation against the dimensions of the chamber. The electron mean free path, λ_{mfp}, may be calculated using the definition $\lambda_{mfp} = 1/(n\sigma)$, where σ is the collision cross-section and n the gas density, with n being determined from the gas pressure using the ideal gas law and assuming a gas temperature of 300 K. Although σ depends on electron energy, we can obtain an sense of the dependence by using the maximum cross section

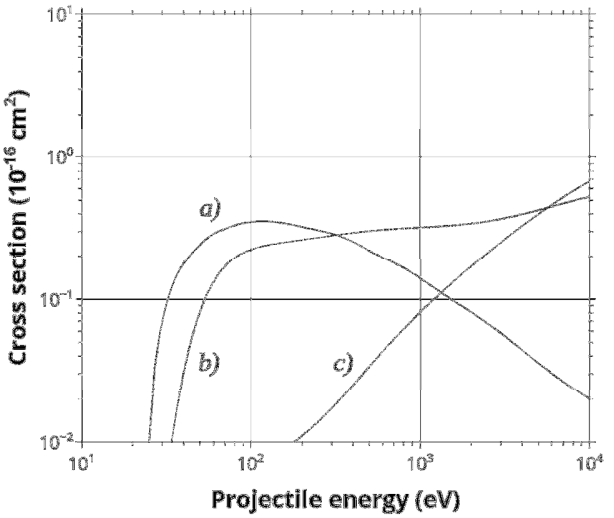

Fig. 11. Cross sections for ionisation of helium by a) electrons, b) ions and c) neutrals. Data taken from [16], [18]-[20].

size (around $3.5\text{x}10^{-17}$ cm^2 for 100 eV electrons [18]) and calculate the minimum ionisation length for a given pressure. Using this method to estimate the ionisation length, we find that it becomes equal to the chamber radius (15 cm) at a pressure of about 8 Pa, and we would expect electron-impact

ionisation to have a negligible effect on the discharge at pressures lower than this value. In this calculation, we have neglected the fact that the electrons have a range of energies, rather than a single value, and we have neglected any gas heating, which would serve to reduce the background neutral density. Even so, in the absence of a mechanism such as a magnetic field that confine electrons and extends their path length, we can conclude that discharges at lower pressures must be sustained by ionisation from ions or energetic neutral species. The value of 8 Pa that we find from this estimation is broadly consistent with the experimentally observed transition between the modes, which occurs in the range of 10-13 Pa.

More generally, this analysis of the emission structure and the broad *E/n* dependences of electron and heavy particle collisional processes, we can conclude that the observed mode structure is due to the discharge being driven principally by electron impact collisions at higher pressures and ion- and neutral-impact collisions at lower pressures.

B. Current-voltage relations

The discontinuities evident in the I-V curves (Figs. 5-7) show a sudden increase in current to be associated with the appearance of the CC mode, and a hysteresis is also found to affect current levels. These characteristics indicate it to be associated with the establishment of a space charge configuration that affords an enhanced efficiency of ionisation. We note the distribution of emission to be similar to that of a hollow cathode discharge, in which an ionisation efficiency results as energetic electrons reaching the boundary of the plasma are reflected by the cathode fall, and so continue to play a role in the discharge. The onset of this 'hollow cathode effect' is accompanied by an abrupt increase in discharge current, and a decrease in operating voltage [21]. Our cathode is considerably more perforated than most hollow cathodes, but the electrostatic electron confinement effect is known to occur in a variety of different types of discharge, including those within grid electrodes. A review of fundamental mechanics of this 'electrostatic trap effect' (ETE) [22] defines four parameters instrumental in determining discharge properties. Two of these describe trapped energetic electron kinetics: the ionisation length, λ_i, describing the mean free path travelled between ionisation events, and range, Λ, the path travelled before losing all kinetic energy; and two characterise geometric properties of the electrostatic trap: an effective width, a, describing the average distance travelled before an electron is reflected at the trap boundary, and length, L, which refers to the average distance travelled by an electron before escaping the trap. It is also noted that the mean ionisation length, as a confined electron loses energy in successive inelastic collisions, may be approximated for electron energies in the range 50 – 500 eV using the same definition for electron mean free path, λ_{mfp}, as for our previous calculation, and an average cross section size, with the average value for λ_i denoted as λ_0. Relations between electron kinetics and trap geometry determine the pressure range at which electron trapping may be significant within a discharge, in that an element of ETE may only operate when Λ exceeds a, and that extinction of the discharge generally occurs as λ_0 exceeds the trap length L. Universal expressions given for a and L are for isotropic electron velocity distributions within cathode geometries of arbitrary form, these are:

$$a = \frac{4V}{S}$$

in which V refers to volume, and S to surface area of the trap, and:

$$L = \frac{4V}{S_0}$$

in which S_0 is the part of S through which electrons may escape, in our case corresponding to ηS, where η is the geometric transparency of the cathode. For our cathode we calculate a to be 4.65 cm, with L only a little larger, at 5.71 cm, due to the relatively high geometrical transparency of 0.81. The average cross section size for electron-impact ionisation of helium derived from the energy-loss approximation given in [22] is $3\text{x}10^{-17}$ cm^2.

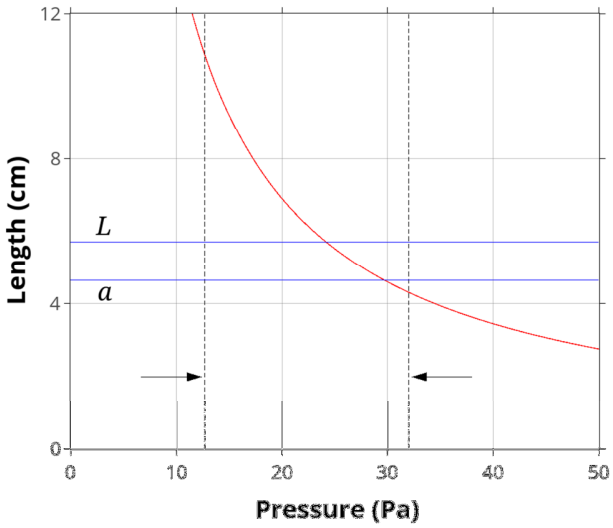

Fig. 12. The curve shows the pressure dependence of mean ionisation length for 50-500 eV electrons at 300 K, compared with a and L as defined in the text. The arrows indicate the regime in which I-V discontinuities are evident.

Fig. 12 shows a comparison of ionisation length, calculated for a gas temperature of 300 K, with a and L over the pressure range of 10-50 Pa. Vertical dashed lines indicate the range of pressures at which I-V discontinuities are apparent. The results indicate the ionisation length to become similar to the trap width, a, at a pressure of around 30 Pa, which is close to the pressure at which discontinuities start to be evident in the I-V relation, at around 32 Pa. This agrees well with the description of the onset of the hollow cathode effect given in [21], in which I-V discontinuities are associated with the ionisation length becoming larger than the cathode width. The relation with Λ given in [22] however suggests that an ETE is significant in the discharge at considerably higher pressures also, consistent with the similar appearance of the mode at pressures of 60 or 70 Pa in helium.

We might expect the low-pressure limit for the CC mode to coincide with the pressure at which the ionisation length becomes similar to the trap length, L; this however occurs at a pressure smaller than 13 Pa, at which the ionisation length is closer to twice the value for L calculated for the cathode. The reason for this discrepancy becomes clear if we consider the

mechanism by which electrons may become significantly confined within such a transparent electrode. The cathode perforations lead to a very small L, and confinement of 'primary' γ-electrons, emitted as ions impact the cathode, will indeed be poor. Any secondary electrons born by ionisations occurring within the sheath will however be confined within the more continuous field structure surrounding the plasma, within which their confined path length will be larger, and this will serve to extend the low-pressure range. We may treat this dynamic by calculating a value for path length within the electrostatic trap, L_T, and then multiplying this by the probability for a primary electron to initially become confined. Assuming an ionising collision to be a necessary and sufficient condition for a primary electron to become confined within the plasma, we expect this probability to be approximated well by L/λ_i, as since we are considering a single first collision, the result will be influenced by the electron energy-dependence of the cross section. Taking this as a free parameter, we have $\lambda_0 \sim LL_T/\lambda_i$ at the extinction pressure, which we re-arrange as $\lambda_i \sim LL_T/\lambda_0$. The cross section size derived from the calculated value for λ_i will then predict an initial electron energy. Expecting confined electrons to be able to escape only via the open end of the cathode, we approximate S_0 as a circle of cathode radius, which provides an estimate for L_T of around 44 cm. At a gas temperature of 300K this predicts a cross section size of 1.43×10^{-17} cm^2, that could theoretically correspond to primary electron energies to either side of the maximum. We observe cathode voltage increases significantly at pressures towards the lower limit, approaching 1000 V, and the magnitude of both cathode voltage and plasma-cathode fall for hollow cathode discharges to generally be similar, and to rise steeply [22] at these conditions. The cross section will therefore correspond to the greater-energy solution, which is consistent with an electron energy a little smaller than 1 keV [18]. This good agreement between theory and experiment supports our identification of the CC mode as a hollow cathode-type plasma, and indicates the approach taken in the analysis to be broadly valid.

To briefly consider the I-V curves obtained from the beam mode discharges; these follow a consistent relation that may be observed to differ slightly from those of the CC mode curves. The beam mode I-V relation is likely to be affected by an increasing secondary electron yield from the cathode, as impacting ion energies increase with voltage. For transition pressures, the parts of the curves obtained prior to the instigation of the CC mode are observed to follow a similar form to the lower-pressure curves, again made more obvious in the helium data by the more marked discontinuity in voltage. This is also consistent with the mode transition representing a change from a higher-pressure regime, in which the discharge is sustained by electron-impact processes, to one in which ions and neutrals are the principally-active species.

V. DISCUSSION

The previous analysis has shown the apparent low-pressure mode structure of the discharge to represent a change in principally-active species within the plasma, from electrons at higher pressures to ions and neutrals at lower pressures.

This identification was made by consideration of the spatial distribution and spectral content of emission from the discharge. Because ions and electrons become reactive at conditions of different E/n, and because significant variation in electric field strength is found within the chamber, a spatial separation of regions in which either species is active may occur at conditions corresponding to the mode transition. This is made visibly apparent in the helium discharge (illustrated in Fig. 4), since excitation caused by the two species results in emission at sufficiently different wavelengths. This localisation of emission caused by the activity of electrons and heavy particles lets the emission structure described by Phelps and Jelenkovic in [14] be clearly observed, and enables a quick diagnosis of active species to be made by eye for these helium discharges. The low-pressure limit for electrons to play a significant role in the sustaining of the discharge has been shown to be affected by the degree of electrostatic confinement afforded by a plasma existing within the grid cathode. In our apparatus the open end of the cathode limits this effect, so that it does not significantly alter the pressure range at which a transition in active species from electrons to heavy particles occurs.

Previous accounts of TCD operation in the literature have also described different modes of operation, identified by Miley et al., and generally referred to as 'jet' and 'star' mode configurations [1], [9], [23]-[26]. The beam mode in our apparatus is visibly similar to the spherical 'star' mode, and it seems likely that these discharges may be analogous. The axial glow that accompanies the mode transition, and that evolves into a narrow axial beam in the beam mode, may be related to features of the 'jet' mode. The colour of these axial structures in helium indicates them to contain energetic electrons. Our analysis has indicated the CC mode to be assisted by an electrostatic trap effect at lower pressures, and one earlier account in the IEC literature [6] also describes a mode occurring at conditions of relatively-high pressure as a hollow cathode-type discharge. More detailed investigation into the relations between modes described in the literature and the mode structure described here, and also the sub-modes not described in this paper, will be the subject of future work.

VI. CONCLUSIONS

In this study, we investigated the characteristics of a cylindrical TCD, operated in helium and argon gas at pressures in the range of 1-100 Pa. We identified the presence of two broad modes of operation, and these became the main focus of investigation.

At higher pressures, above about 2-3 Pa in argon and 12-15 Pa in helium, the discharge operates in a stable mode in which emission is observed almost solely from the interior of the cylindrical cathode. We called this mode of operation the cathode-confined (CC) mode. Measurement of current-voltage characteristics and analysis of plasma emission led to the conclusion that this represents a discharge mode in which (i) electron-impact collisions are the primary driving mechanism,

and (ii) a hollow cathode effect is important in sustaining the mode.

At lower operating pressures, we observed a stable mode of operation in which the plasma emission is characterised by radial beams of strong emission, passing through the apertures of the grid electrodes and, for high current conditions, reaching the chamber walls. While some emission is observed inside the cylindrical cathode, the overall emission is dominated by the radial beams. We called this the beam mode. Analysis of plasma emission and consideration of collision dynamics led to the conclusion that collisions processes involving energetic ion and neutral species are important in sustaining this discharge mode, and that electron-impact collisions are by comparison relatively unimportant.

The identification of this mode structure is a particularly useful result, and the separation into clearly-defined modes, of discharge regimes in which electrons and heavy particles are principally reactive, is a most convenient property of this TCD configuration. As an artefact of the different *E/n* regimes at which electrons and heavy particles gain reactive energies, the mode structure therefore represents a progression of fundamental discharge properties that will be quite universal, and the beam mode constitutes the form this heavy particle discharge takes in our apparatus. The recognition of the role played by the hollow cathode effect in the CC mode is also an important result, as this effect becomes significant at the boundary between the two modes. An understanding of the processes that cause the CC mode to appear is necessary for the engineering of a stable ion- and neutral-driven source.

Although in this study we focused on the two main discharge modes, we also noted the presence of other modes that appeared in more restricted operating ranges. These require further investigation and will be the subject of future work.

REFERENCES

[1] R. M. Meyer, M. A. Prelas, and S. K. Loyalka, "Experimental Observations of a Transparent Cathode Glow Discharge," *IEEE Trans. Plasma Sci.,* vol. 36, no. 4, pp 1881-1889, Aug. 2008.

[2] W. C. Elmore, J. L. Tuck, and K. M. Watson, "On the Inertial Electrostatic Confinement of a Plasma," *Phys. Fluids,* vol. 2, no. 3, pp. 239-246, May 1959.

[3] O. Lavrent'ev *et al.*, "Jenergiya i plotnost'ionov v jelektromagnitnoj lovushke," *Ukrain Fiz. Zh.,* vol. 8, pp. 440-445, 1963.

[4] P. T. Farnsworth, "Electric Discharge Device for Producing Interactions between Nuclei," U.S. Patent 3258402, Jun. 28, 1966.

[5] P. T. Farnsworth, "Method and Apparatus for Producing Nuclear-Fusion Reactions," U.S. Patent 3386883, Jun. 4, 1968.

[6] R. L. Hirsch, "Inertial Electrostatic Confinement of Ionized Fusion Gases," *J. Appl. Phys.,* vo. 38, no. 11, pp. 4522-4534, Oct. 1967.

[7] G. H. Miley and J. Sved, "The IEC star-mode fusion neutron source for NAA—status and next-step designs," *Appl. Rad. Isotopes,* vol. 53, no. 4, pp. 779-783, Nov. 2000.

[8] J. W. Weidner *et al.*, "Production of 13 N via Inertial Electrostatic Confinement Fusion," *Fus. Sci. Tech.,* vol. 44, no. 2, pp. 539-543, 2003.

[9] G. H. Miley *et al.,* "Thruster design for IEC-based spacecraft propulsion," in *ANSETM - 2005 Space Nuc. Conf.,* American Nuclear Society, 2005, pp. 775-780.

[10] L. Blackhall and J. Khachan, "A simple electric thruster based on ion charge exchange," *J. Phys. D: Appl. Phys.,* vol. 40, no. 8, pp. 2491, Apr. 2007.

[11] T. Thorson, R. Durst, R. Fonck, and A. Sontag, "Fusion reactivity characterization of a spherically convergent ion focus," *Nuc. Fus.,* vol. 38, no. 4, pp. 495, Apr. 1998.

[12] O. Shrier *et al.,* "Diverging ion motion in an inertial electrostatic confinement discharge," *Phys. Plasmas,* vol. 13, no. 1, pp. 012703, Jan. 2006.

[13] J. Khachan, and A. Samarian, "Dust diagnostics on an inertial electrostatic confinement discharge," *Phys. Lett. A,* vol. 363, no. 4, pp. 297-301, Apr. 2007.

[14] B. Jelenković and A. Phelps, "Excitation in low-current discharges and breakdown in He at low pressures and very high electric field to gas density ratios *E/n," Phys. Rev. E,* vol. 71, no. 1, pp. 016410, Jan. 2005.

[15] P. Hartmann *et al.* "Effect of different elementary processes on the breakdown in low-pressure helium gas," *Plasma Sources Sci. Tech.,* vol. 9, no. 2, pp. 183, May 2000.

[16] Y. V. Ralchenko *et al.,* "Cross Section Database for Collision Processes of Helium Atom with Charged Particles. 1. Electron Impact Processes," INIS, Japan, Oct. 2000.

[17] R. Okasaka *et al.,* 1987. Excitation cross sections in He -He collisions. I. Excitation function and potential curve crossing, *J. Phys. B: Atom. Mol. Phys.*, vol. 20, no. 15, pp. 3771, Aug. 1987.

[18] LXCat database. Available: https://fr.lxcat.net/home/ (retrv'd. 31/07/18)

[19] Aladdin database. Available: https://www-amdis.iaea.org/ALADDIN/ (retrv'd. 31/07/18)

[20] H. C. Hayden and N. G. Utterback, "Ionization of helium, neon, and nitrogen by helium atoms," *Phys. Rev.*, vol. 135, no. 6A, p. A1575, Sep. 1964

[21] E. Oks, "Low-pressure discharges for plasma electron sources," in *Plasma cathode electron sources: physics, technology, applications.* New York, NY, USA: John Wiley & Sons, 2006, ch. 1, sec. 1.1, pp. 2-6.

[22] V. Kolobov and A. Metel, "Glow discharges with electrostatic confinement of fast electrons," *J. Phys. D: Appl. Phys.,* vol. 48, no. 23, pp. 233001, Jun. 2015.

[23] G. H. Miley *et al.,* "Inertial Electrostatic Confinement Neutron/Proton Source," in *Dense Z-Pinches: 3rd Intl. Conf.*, AIP Publishing, 1994, pp. 675-689.

[24] G. H. Miley *et al., "*Discharge characteristics of the spherical inertial electrostatic confinement (IEC) device," *IEEE Trans. Plasma Sci.,* vol. 25, no. 4, pp. 733-739, Aug. 1997.

[25] R. M. Meyer, M. A. Prelas, and S. K. Loyalka, "Ion flow convergence in spherical inertial electrostatic confinement devices," *Phys. Plasmas,* vol. 15, no. 2, p. 022105, Feb. 2008.

[26] M. Yousefi, V. Damideh, and H. Ghomi, "Low-energy electron beam extraction from spherical discharge," *IEEE Trans. Plasma Sci.,* vol. 39, no. 11, pp. 2554-2555, Jul. 2011.

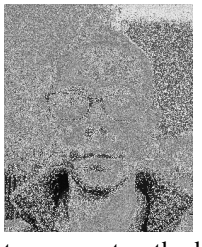

Tom Hardiment received a BSc in Physics from Heriot-Watt University, UK, in 2012, the MSc degree in High Power RF Science and Engineering from University of Strathclyde in 2013, and the PhD degree from University of Liverpool, UK, in 2018, studying operating characteristics of a low-pressure transparent cathode discharge. He is currently working as a Research Associate at the University of Liverpool, developing an atmospheric plasma source for surface sterilisation applications.

His research interests include the development of IEC technology for both fusion and non-fusion applications, and

the understanding of fundamental principles for engineering of plasma sources.

Mark D. Bowden received a BSc degree in Physics from the University of Sydney, Australia, in 1987, and a PhD degree from the same university in 1991 on the topic of laser development and their applications for the study of fusion plasma.

In 1991, he started at Kyushu University, Japan as a JSPS Postdoctoral Fellow, becoming a Research Associate in 1993 and Associate Professor in 1998, specializing in development of measurement techniques for low-pressure gas discharges, and applications such as plasma etching. In 2001, he moved to the Faculty of Applied Physics at Eindhoven University of Technology, the Netherlands, working on industrial projects with Phillips Lighting and specifically on plasma breakdown. In 2005, he moved to the Open University in the UK, and in 2013 he moved to his current position at the University of Liverpool, UK. His research interests continue to be fusion, gas discharges, plasma breakdown, and the development of measurement techniques for these systems.